Performance of Flash Lidar with real-time image enhancement algorithm for landing hazard avoidance

Farzin Amzajerdian[1], Paul Brewster[2], Byron Meadows[3], Rafia Haq[4]
NASA Langley Research Center, Hampton, Virginia 23681, USA

Alexander Bulyshev[5], Guoqing Shen[6]
Coherent Applications Inc, Hampton, Virginia 23666, USA

Stefan Bieniawski[7], Brandon P. Smith[8], and Devin Kipp[9]
Blue Origin, Kent, Washington 98032, USA

Performance of a 3-D imaging flash lidar employing a novel super-resolution algorithm is characterized by a series of static and dynamic tests. A gantry test of this lidar in which the lidar was placed in an instrumented moving basket above a calibrated hazard field proved an excellent demonstration of hazard avoidance capabilities. Results of the gantry test are reported and potential of flash lidar utilizing super-resolution algorithm for future landing missions are explained.

I. Introduction

Flash lidar is recognized as one of the leading sensor technologies for enabling onboard hazard detection and avoidance required by many lunar landing missions including manned missions.[1-3] Interest in flash lidar technology stems from its ability to record full 3-D images with a single laser pulse, freezing the scene on every frame by removing all motion of the transmitter/receiver platform. Unlike more conventional topographic imaging lidar systems that generated 3-D images by scanning the laser beam across the scene and measuring the time of arrival for each returned laser pulse, the flash lidar records a full 3-D image frame by illuminating the scene with a single laser pulse and imaging the scene onto one focal plane array (FPA). Each pixel in the FPA takes independent measurements of the lidar pulse time of flight to the target. Therefore, the flash lidar permits much higher frame rates without any blurring or inaccuracies due to platform motion.

Potentials of flash lidar technology have been demonstrated through aircraft flight tests and most notably, onboard Morpheus, a terrestrial rocket-powered vehicle.[4-6] Morpheus flight test campaign was conducted at the hazard field specifically constructed for this purpose near the north end of the Shuttle Landing Facility (SLF) runway at NASA

---

[1] EDL Lidar Sensors Lead, LaRC Remote Sensing Branch, Engineering Directorate
[2] Lead System and Software Engineer, LaRC Flight Software Branch, Engineering Directorate
[3] Project Manager, LaRC Remote Sensing Branch, Engineering Directorate
[4] Software Engineer, LaRC Flight Software Branch, Engineering Directorate
[5] Lidar Signal Processing Lead, LaRC Remote Sensing Branch, Engineering Directorate
[6] Lead Electro-Optical Engineer, LaRC Remote Sensing Branch, Engineering Directorate
[7] Tipping Point Principal Investigator, Blue Origin
[8] Tipping Point/Hazard Avoidance Lidar Lead, Blue Origin
[9] Tipping Point/Flash Lidar Lead, Blue Origin

Kennedy Space Center (KSC). The hazard field was a 100 m x 100 m area simulating a challenging lunar terrain and consists of realistic hazard features (rock piles and craters) and designated landing areas. Flash lidar operating in closed-loop with the vehicle Guidance, Navigation, and Control (GN&C) system, was able to detect the hazards and provide the necessary data for the vehicle to land at the identified safe location.

The hazard detection requirements depend on the landing system design and mission objectives. Many factors must be considered to define the size of surveyed area, minimum detectable hazard size, and the minimum altitude at which the safe landing location is identified and reported to the GN&C system. Lander descent trajectory divert maneuver capability and structural properties (clearance from ground, center of gravity, etc.) are some of the considerations for defining the operational requirements of hazard detection sensor. In order to guide the technology development, a baseline performance for the hazard detection and avoidance sensor has been developed based on robotic and manned lunar lander concepts under consideration. In short, we aim to generate a Digital Elevation Map (DEM) of an approximately 70 m x 70 m area and to detect 20 cm radius hazards before reaching 500 m altitude above ground.

The current Flash Lidar has a 128 x 128 pixels detector array that is insufficient to meet the stated baseline performance. Adjusting the Field-Of-View (FOV) of the Flash Lidar to cover 70 m x 70 m area will result in a Ground Sample Distance (GSD) of 55 cm (= 70 m/128), much greater than 20 cm hazard radius. The GSD must be approximately half the hazard radius for reliable operation. To overcome this shortcoming, the past demonstration flight tests used a mechanical gimbal to scan the target area and stitch a number of individual image frames with sufficiently small FOV and GSD. However, accommodation of a relatively large mechanical gimbal on landing vehicles, such as the one used for Morpheus flight test, is very challenging or even impractical. For this reason, we employ a Super-Resolution (SR)[7-9] technique to eliminate the mechanical gimbal. In SR operation, the lidar FOV is enlarged to cover the whole area of interest and then a sequence of image frames of the same scene, taken from different positions and look angles, are blended to achieve the desired resolution.

This paper describes the performance of flash lidar employing real-time SR image enhancement algorithm in meeting landing hazard detection and avoidance requirements. A dynamic test was devised to demonstrate the capabilities of flash lidar and pave the path for development of a prototype unit and conducting aircraft flight tests simulating landing operation.

II. Flash Lidar Sensor Description

The principal of a flash lidar sensor system is illustrated in Figure 1. The flash lidar uses a two-dimensional detector array to detect a laser pulse return from the target. The detector's Readout Integrate Circuit (ROIC) measures the laser pulse time of arrival of each individual pixel simultaneously, thus each flash of the laser generates a 3-D image of the target illuminated by the laser beam.[10-11] In older, more conventional imaging lidar systems, the laser beam is scanned over the targeted area in a raster pattern and a single detector is used to detect consecutive pulses. Thus many laser pulses are required to cover the target area and generate a multi-pixel image with sufficient resolution. For example, generating a 3-D map of a 70 m X 70 m area with 10 cm resolution (0.5M pixels) using a typical 10 kHz laser repetition rate will take 50 seconds which is not practical for a landing scenario.

Another major challenge of a scanning system is controlling the laser beam pointing from a moving platform and then estimating the laser spot position in the target area for each transmitted pulse. By recording a full 3-D image with a single laser pulse, the flash lidar provides a much higher image frame rate, eliminating the need for a fast laser beam scanning mechanism, and mitigates the effects of platform motion.

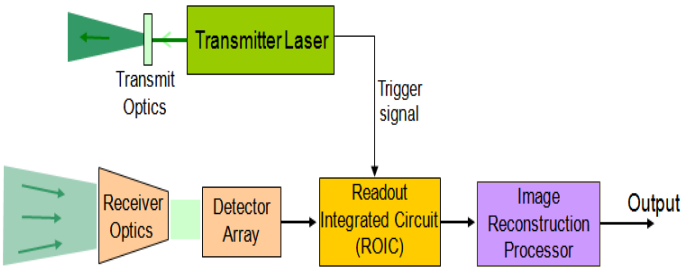

Fig. 1 Schematic of Flash Lidar Sensor System.

III. Landing Operational Concepts and Requirements

In addition to Hazard Detection and Avoidance (HDA), flash lidar can perform three other essential functions during the descent and landing phases: Altimetry, Terrain Relative Navigation (TRN)[12], and Hazard Relative Navigation (HRN)[13]. Figure 2 illustrates flash lidar operation in the context of a lunar landing. The lidar begins its

operation at about 20 km above the ground after thruster rocket firing is initiated. At this stage, the lidar transmitter beam is focused to illuminate only a few pixels in the center of the detector array to measure range to the ground. Reducing the divergence of the lidar transmitter beam to a fraction of its receiver field of view increases its operational slant range to well over 20 km from a nominal 1 km. The ground-relative altitude measurements provided by the flash lidar reduce the vehicle position error significantly since the Inertial Measurement Unit (IMU) suffers from significant drift over the travel time from the Earth. Position error at the initiation of de-orbit and power descent can be more than 1 km, which may be reduced to a few hundred meters with accurate ground-relative altitude data.

When the altitude drops to about 10 km, the lidar beam is expanded to illuminate approximately two hundred detector pixels. In this phase of its operation, the flash lidar generates relatively low-resolution elevation data of the terrain below which are subsequently compared with stored maps having known surface features such as large craters. This process, referred to as TRN, further reduces the vehicle's relative position error from hundreds of meters to tens of meters. From about 1 km altitude, the flash lidar operates with its full field of view to perform the HDA function by generating high-resolution elevation maps of the landing area. These elevation maps are then processed to identify hazardous features such as rocks, craters, and slopes, and to determine the most suitable landing location before reaching 500 m altitude. The flash lidar continues to update the map in order to establish a trajectory toward the selected landing location. This phase of flash lidar operation is referred to as HRN. The flash lidar operation terminates at approximately 20 m above the ground before the vehicle thrusters create a dust plume.

The operational scenario of Figure 2 serves as a guideline for the lidar technology development and the operational altitudes for each of the four functions may vary depending on the descent trajectory, vehicle divert capabilities, landing area terrain, required landing ellipse precision, and other mission requirements. The performance parameters of flash lidar is essentially established by the HDA requirements. The HDA performance goal is to map a 70 m x 70 m area with 10 cm Ground Sample Distance (GSD) that is a 0.5M pixels digital elevation map (DEM). However, a flash lidar with a 0.5 M pixels detector array is impractical for the foreseeable future. This type of high-resolution sensor will require significant advancements in Avalanche Photodetector (APD) arrays and the associated Readout Integrated Circuit (ROIC) chips. In addition to more than an order of magnitude more pixels, the hybridized detector array and ROIC must achieve a considerably smaller pitch size and much lower noise and higher gain, well beyond the current state of technology of 16.4 k pixels, in order to allow for a reasonable laser pulse energy and receiver aperture size.

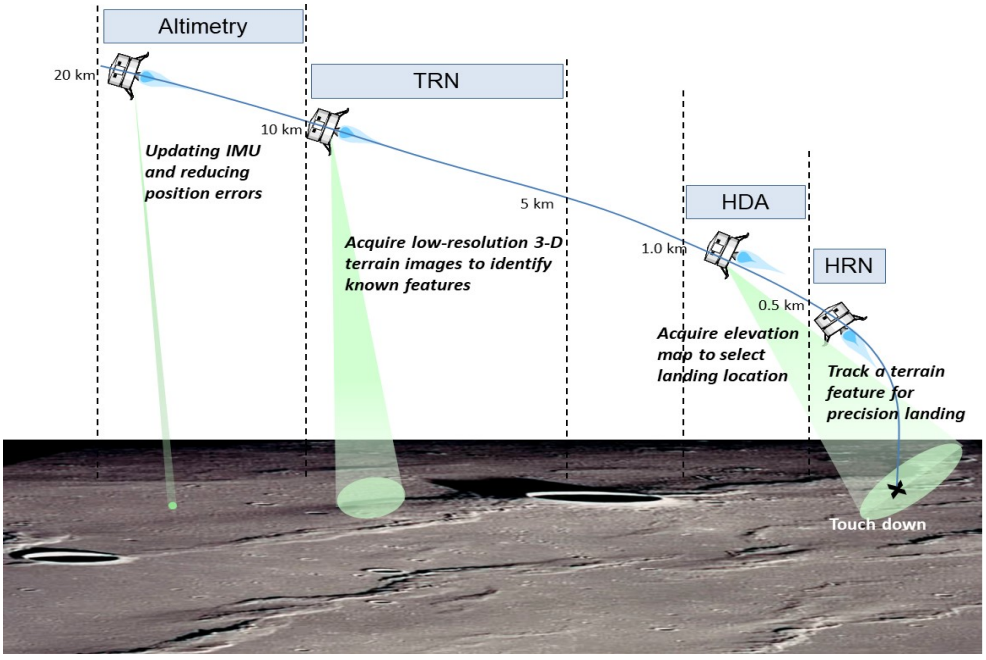

Fig. 2 Flash lidar landing operational concept.

IV. Super Resolution Technique

The Super-Resolution (SR) technique, developed by NASA Langley Research Center (LaRC), eliminates the need for a large mechanical gimbal for scanning the lidar and allows for a compact sensor capable of meeting the general requirements for precision and safe landing as described in previous section. SR takes advantage of sub-pixel shifts

between multiple, low-resolution images of the same scene to construct a higher resolution image. SR is a well-established technique for enhancing two-dimensional (2-D) images, and over the years a large number of algorithms have been developed for processing intensity images produced by different types of imaging systems. With the emergence of flash lidar technology, several researchers studied the potential application of the SR technique to this data source. However, these earlier efforts could only achieve 3-D image enhancements when the camera was subjected to a controlled motion within a tightly constrained envelope, with or without image registration.[15-17] The requirement to tightly constrain camera motion in these techniques precluded their implementation on landing vehicles which typically undergo significant excursions in position and orientation. An additional limitation of the past work is that they require external sensors to provide the camera's position and pointing angle. The 3-D SR algorithm, developed by NASA, can create a DEM with a digital magnification factor of five to eight in real-time while providing all six components of the lidar's position and orientation vector.[9]

The SR algorithm utilizes a modified back-projection method and an iteration process to reconstruct a 3-D surface for an arbitrary look-angle. The algorithm calculates the six-degree-of-freedom (6-DOF) relative state vector (lidar instrument position coordinates and three components of pointing angle) using consecutive image frames. Determination of the instrument state vector is crucial for registration of individual frames prior to combining them to generate a SR image using an inverse filter algorithm. The state vector data provided by this algorithm may also be used by the vehicle for precise navigation to the intended destination. In addition to eliminating the need for a scanning gimbal, the SR has several important advantages compared with stitching individual image frames. The SR technique lowers range measurement noise, eliminates bad pixels, and reduces DEM acquisition time (fewer image frames).

Performance of the SR was analyzed using a high fidelity Matlab model showing that a digital magnification factor of five to eight (25X to 64X number of original image pixels) can be achieved by processing 20 consecutive flash lidar frames. The simulations were based on a flash lidar operating at 20 Hz frame rate, acquired from Advanced Scientific Concepts.

Recently, under a NASA Tipping Point project led by Blue Origin, we implemented the SR algorithm on a Graphics Processing Unit (GPU) capable of real-time processing of flash lidar images. The integrated flash lidar/GPU was tested from a moving platform at NASA LaRC's gantry facility. Test results were in excellent agreement with the projected performance indicating 25X image enhancement (0.4M pixels) and 2.5X reduction in range noise. Analytical models indicate that an image enhancement of up to 64X (1.0M pixels) is feasible by improving transmitted far-field beam pattern.

V. Dynamic Gantry Test

A series of tests were conducted on the flash lidar in laboratory and at NASA LaRC lidar test range over horizontal paths in both static and dynamic setups. These tests provided valuable data for characterizing the lidar performance and conducting design trades for a protype unit. However, lack of an extended target filling the whole FOV of the receiver from a moving platform impeded full lidar characterization and validation of SR image enhancement and hazard classification algorithms. The gantry facility at NASA-LaRC provided for a convenient and low-cost opportunity for testing of the flash lidar integrated with real-time SR. The gantry test is not a substitute for aircraft flight tests due to limited height and restricted motions, but an excellent setup for characterizing the lidar and image processing algorithm.

For the gantry test, the flash lidar was placed inside an instrumented basket designed to be lifted by the gantry tether. The gantry facility, shown in Figure 3, can lift the instrument platform to 64 m height above the ground and introduce a vertical motion with up to 10 m/min. Figure 3 also shows the instrument basket with flash lidar mounted to its side looking down at the ground.

A hazard field consisting of rectangular and hemispherical objects with different sizes, from 5 cm to 1 m, was assembled under the gantry structure. The target objected were coated for diffuse reflection similar to natural targets. The reflectivity of the target objects and samples of the concrete surface were measured prior to tests. Figure 4 shows a top view the "hazard field" and the instrument basket. A laser tracker instrument was used to measure the size and location of each object to about 1 mm precision for generating a truth map.

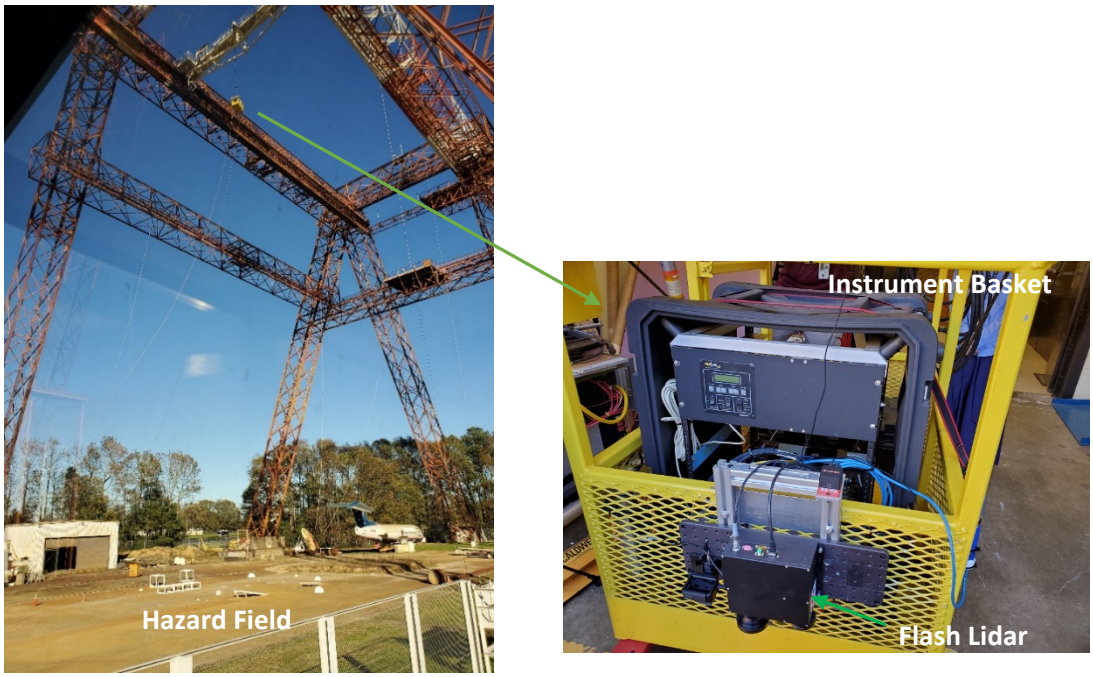

Fig. 3 (left) NASA LaRC Gantry Facility used for testing a flash lidar integrated with real-time SR processor. (right) Instrument basket housing the flash lidar and support equipment.

A. Gantry Test Results

The following test results describes the image enhancement achieved by the SR algorithm and quantifies the flash lidar performance parameters relevant to HDA. The lidar was operating at 20 Hz frame rate and all the SR DEMs were generated by processing 20 individual range image frames, i.e., SR DEMs were generated at 1 Hz rate. The tests were conducted with a 15 degrees Field Of View (FOV) receiver lens that covers 15.8 x 15.8 m area on ground from 60 m height with a corresponding GSD of 12.3 cm.

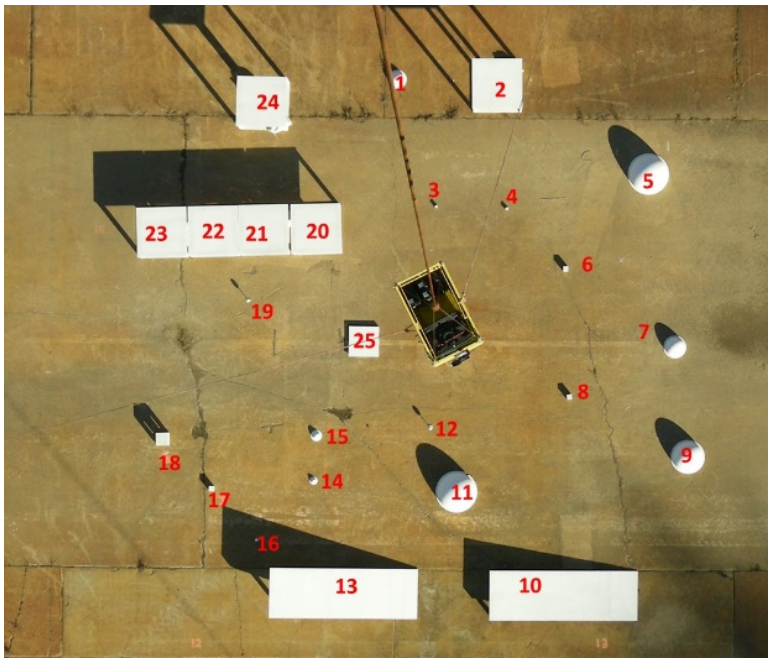

Fig. 4 Hazard field with different shapes and sizes objected with known reflectivity.

Figure 5 is an example of lidar image frames of the hazard field compared with a SR DEM of the same area. The single frame image shows a significant number of dark pixels that have not provided range data. Most of the dark pixels are unfunctional detector elements due to manufacturing yield of focal plane arrays and a few are random pixels that simply have not receive enough photon to generate a range data. As shown in this example, SR algorithm recovers almost all dark pixels by averaging multiple frames. This is an important feature of the algorithm that mitigates the risk of false negative in hazard detection.

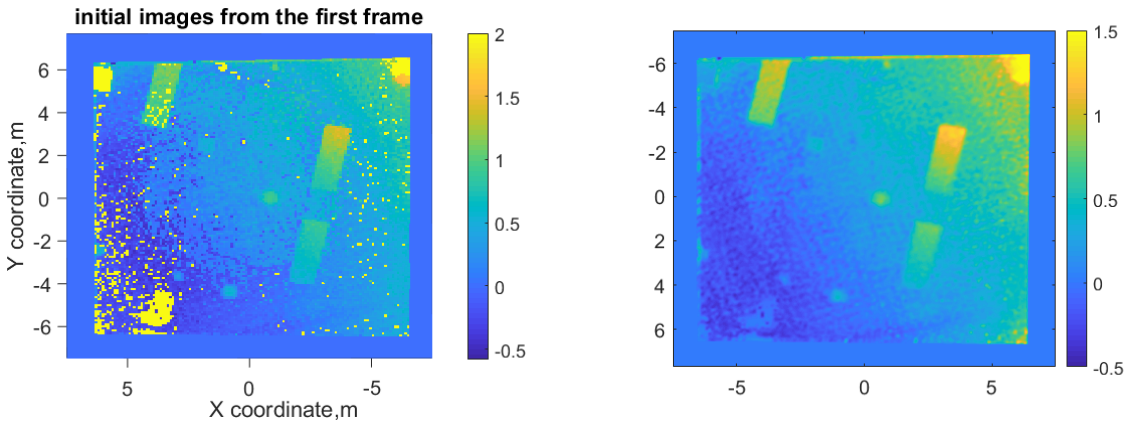

Fig. 5 DEM restored from a single frame on the left, DEM restored using 20 frames on the right. Yellow dots are the dark pixels.

Figure 5 shows a smoother DEM as opposed to a pixelated image which points to higher resolution. Resolution enhancement is quantified in Figure 6 where a section of the DEM is exploded to show the gaps between four square tables. Resolution can be defined as the minimum distance between two objects for which they can be distinguished from each other. If the distance between them is reduced below the image resolution, they will be seen as a single object. There are a number of techniques for determining the image resolution numerically. The most common technique is Rayleigh Criterion. The Rayleigh Criterion works well for 1-D cases, however its application to 2-D and 3-D images become complicated and may not be useful. For this reason, the digital image magnification is used to quantify the 3-D SR performance. To quantify the algorithm's resolution performance, four table-like objects (# 20,21,22,23) were placed with 1, 3, and 5 cm spacing between them. For the example of Figure 6, the SR algorithm was able to detect the 3 cm and 5 cm gaps. So, we can claim that achieved resolution is 1/4 of 12 cm pixel size and thus a digital magnification of at least 4X is achieved. This assessment is based on the assumption that a single frame image has a resolution equal to the pixel size. This is a popular notion, but it is not actually true. In reality, the resolution is at least 2 pixel sizes and more likely 3 pixel sizes depending on the image noise. Therefore, our estimation of 4X digital magnification is very conservative.

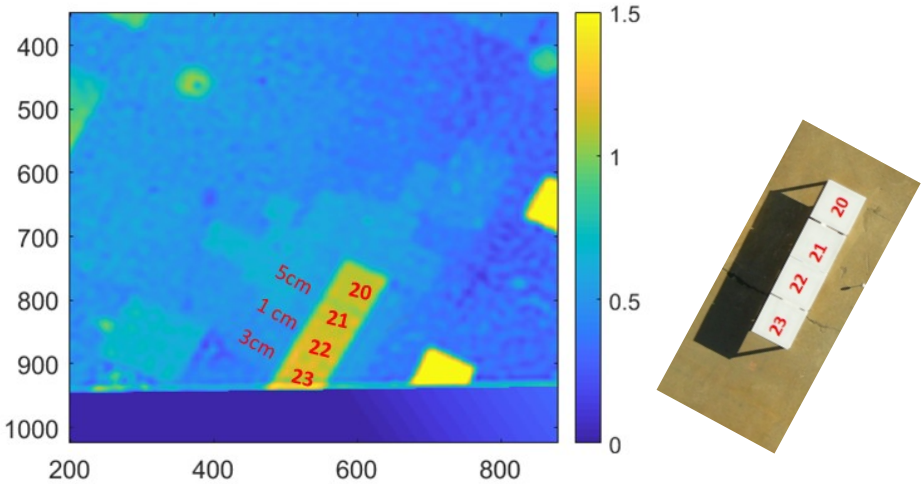

Fig. 6. Gaps between objects 20 and 21 (5cm) and between tabes objects 23 and 22 (3cm) are resoved by the SR algorithm. Gap between objects 21 and 22 (1cm) cannot be resolved.

An important feature of SR algorithm is improved range measurment precision. Figure 7 shows the projected range data along a line in an area of the hazard field without any of the target objects corresponding to a single frame DEM and a SR DEM. Statistical analysis shows that SR algorithm reduces random noise by approximately 2.5X from 7 cm to about 3 cm. However, the noise should have reduced by 4.5X if range noise was completely random. This indicates that the lidar range error has a systematic error component which might be possible to eliminate by improving the transmitter optics and generate a more uniform laser beam pattern on the ground.

The following table summarizes the real-time SR algorithm performance demonstrated by the gantry test.

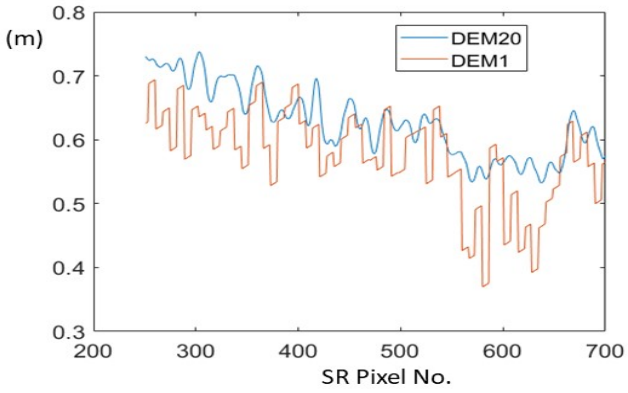

Fig. 7 Linear range profile of DEM over a flat area free of target objects.

• Linear magnification (lateral resolution enhancement)	> 4X (effective # of pixels > 0.26 M)
• Range resolution (vertical resolution enhancement)	2X (4 cm)
• Range noise reduction	2.5X (3 cm)
• Rate of SR DEMs	1 Hz rate
• Dark pixels recovery	> 99%
• Vehicle relative position precision	4 cm
• Vehicle relative attitude precision	0.03°

Perhaps the most meaningful figure of merit for the lidar is the the smallest hazard that can be detected given the slant distance to the landing location and size of the surveyed area. As shown in Figure 8 below, the 5 cm cube targets were detected in the generated DEM from 44 m distance. The lidar pixel size is 9.1 cm from this height. Therefore, it can be concluded that the smallest detectable hazard size is close to half the lidar pixel size. Without the SR, the smallest detectable hazard is at least 2 pixels.

It should be noted that the flash lidar performance utilizing the SR algorithm can be further improved by optimizing the spatial profile of the laser beam illuminating the target area. It is expected to achieve better than 0.5 pixel hazard detection with better than 99% probability by careful design of lidar system.

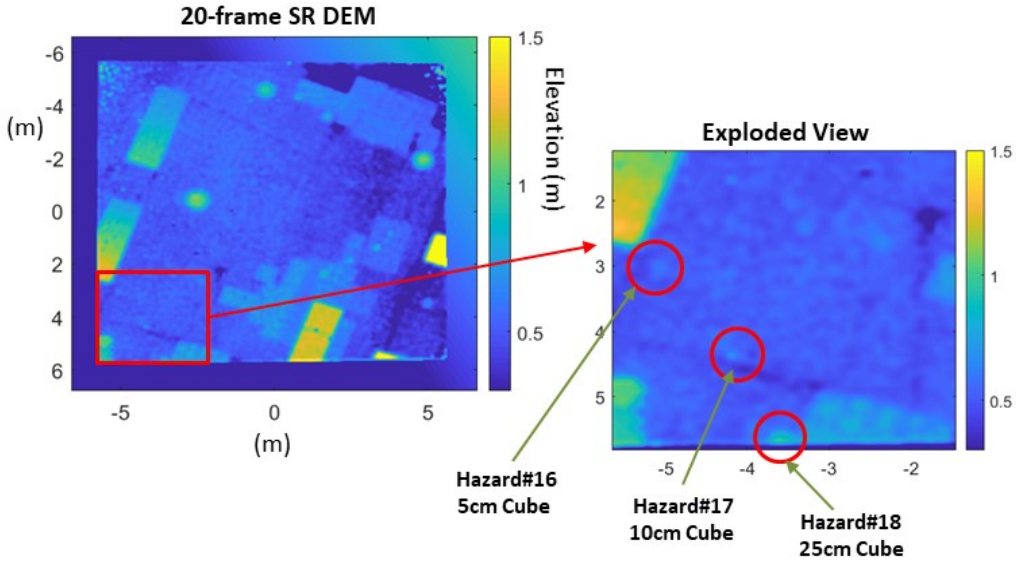

Fig. 8 Samllest detectable hazard with SR algorithm is 0.5 pixel size as opposed to > 2 pixels for a signle range image.

VI. Conclusion

A series of tests including a dynamic test at NASA LaRC's gantry facility were conducted to demonstrate the viability of the 3-D imaging flash lidar employing SR algorithm as an onboard landing hazard avoidance sensor. Flash lidar technology, generating 3-D image frames at video rates, can also perform critical Altimetry, TRN, and HRN functions in addition to HDA. Earlier flash lidar demonstration utilized a relatively large mechanical gimbal to scan the lidar FOV across the targeted area and mosaic the individual frames to achieve the desired resolution. Image enhancement SR algorithm, developed at NASA LaRC, eliminates the need for a mechanical gimbal allowing for a relatively compact sensor that can be accommodated by any landing vehicle.

The results of the gantry test, as described in this paper, show that the flash lidar 3-D images can be significantly enhanced in both resolution and noise by the SR algorithm. The test results indicate greater than 4X image magnification and 2.5X lower range noise by applying the SR algorithm. The algorithm generated 0.26M pixels DEMs at 1 Hz using a commercial flash lidar system. Characterization of the flash lidar identified a number of design improvements that can potentially increase the image magnification to 8X and achieve 1.0M pixels DEMs. This would be more than sufficient to satisfy almost any landing scenario being considered. A prototype unit incorporating much of the identified upgrades has been designed that can operate from more than 1 km distance with its full FOV.

Acknowledgments

This work was funded by the NASA's Tipping Point Program. The authors would like to acknowledge the support of NASA Space Technology Mission Directorate (STMD)-Game Changing Development (GCD) office. We also would like to thank Kevin Somervill, STMD/Technical Integration Manager for Extreme Environments, for his guidance and support.

References

[1] Amzajerdian, F., Vanek, M. D., Petway, L. B., Pierrottet, D. F., Busch,G. E., Bulyshev, A., "*Utilization of 3-D Imaging Flash Lidar Technology for Autonomous Safe Landing on Planetary Bodies,*" SPIE Proceeding Vol. 7608, paper no 80, 2010.

[2] Farzin Amzajerdian, Vincent E. Roback, Alexander E. Bulyshev, Paul F. Brewster, William A. Carrion, Diego F. Pierrottet, Glenn D. Hines, Larry B. Petway, Bruce W. Barnes, and Anna M. Noe, "*Imaging flash lidar for safe landing on solar system bodies and spacecraft rendezvous and docking*," Proc. SPIE Vol 9465, 2015.

[3] Farzin Amzajerdian, Vincent E. Roback, Alexander Bulyshev, Paul F. Brewster, Glenn D. Hines, "*Imaging Flash Lidar for Autonomous Safe Landing and Spacecraft Proximity Operation,*" AIAA SPACE Forum, (AIAA 2016-5591), 2016

[4] Carson III, J. M., Robertson, E. A., Trawny, N., and Amzajerdian, F., "*Flight Testing ALHAT Precision Landing Technologies Integrated Onboard the Morpheus Rocket Vehicle*," Proc. AIAA Space 2015 Conf., paper no. 4417, 2015.

[5] Nikolas Trawny, Andres Huertas, Michael Luna, Carlos Y. Villalpando, Keith E. Martin, John M. Carson III, Andrew E. Johnson, Carolina Restrepo, Vincent E. Roback, "*Flight testing a Real-Time Hazard Detection System for Safe Lunar Landing on the Rocket-powered Morpheus Vehicle*," Proc. of AIAA Science and Technology Forum and Exposition, 2015.

[6] Vincent E. Roback , Diego F. Pierrottet, Farzin Amzajerdian, Bruce W. Barnes, Glenn D. Hines, Larry B. Petway, Paul F. Brewster, Kevin S. Kempton, and Alexander E. Bulyshev, "*Lidar sensor performance in closed-loop flight testing of the Morpheus rocket-propelled lander to a lunar-like hazard field*," Proc. of AIAA Science and Technology Forum, 2015.

[7] Bulyshev, Alexander; Amzajerdian, Farzin; Roback, Vincent E; Hines, Glenn; Pierrottet, Diego; Reisse, Robert, "*Three-dimensional super-resolution: theory, modeling, and field test result*s," Applied Optics, Vol. 53, pp.2583-2594, 2014

[8] Bulyshev, D.F. Pierrottet, F. Amzajerdian, G.E. Busch, M. Vanek, and R. Reisse, "*Processing of three-dimensional flash lidar terrain images generating from an airborne platform*," Proc. SPIE Vol. 7329, 2009.

[9] Alexander Bulyshev, Farzin Amzajerdian, Eric Roback, Robert Reisse, "*A super-resolution algorithm for enhancement of flash lidar data: flight test results*," Proc. SPIE Vol. 9020, 2014

[10] Stettner, R., Bailey, H., and Silverman, S., "*Three Dimensional Flash Ladar Focal Planes and Time Dependent Imaging*," International Symposium on Spectral Sensing Research, Bar Harbor, Maine, 2006.

[11] Stettner, R., "*Compact 3D Flash LIDAR video cameras and applications*," Proc. of SPIE Vol. 7684, 768405, 2010.

[12] Johnson, A.E., and Montgomery, J., "*An Overview of Terrain Relative Navigation for Precise Lunar Landing*," IEEE Aerospace Conference, 2008.

[13] Epp, C. D., Robertson, E. A., and Brady, T., "*Autonomous Landing and Hazard Avoidance Technology (ALHAT)*," IEEE Aerospace Conference, paper #1644, 2008

[14] Rosenbush, T. Hong, and R. Eastman, "*Super-resolution enhancement of flash LADAR range data*," Proceedings of SPIE, Unmanned/Unattended Sensors and Sensors Networks IV, **6736**, 673614-1 – 673614-10, 2007.

[15] S. Hu, S. S. Young, T. Hong, J. Reynolds, K. Krapels, B. Miller, J. Thomas, and O. Nguyen, "*Super resolution for flash LADAR imagery*," Applied Optics **49**(5),772–780, 2010.

[16] S. Hu, S. Young, T. Hong, J. Reynolds, K. Krapels, B. Miller, J. Thomas, and O. Nguyen, "*Super-Resolution for flash LADAR data,*" Proceedings of SPIE vol. 7300, 2009.